The fMRI Study of Creative Thinking in Art Design

Yunxia Qu[1] and Nan Zhao[2,*]

[1]Department of Modeling, College of Art and Design, Shaanxi Institute of Garment Engineering, Xi'an 71000, China, quyunxia123@139. Com
[2]Department of Film, Yantai University, Yantai 264000, China, 352918603@ytu.edu.cn

communication author: Nan Zhao, 352918603@ytu.edu.cn

Abstract. Magnetic resonance imaging (MRI) has rich contrast information, high resolution, can be sliced in any direction, and has no radiation damage, which plays an important role in clinical diagnosis. The research on the brain mechanism of human creative thinking is one of the hot spots, and it has always attracted the attention of various fields. Intelligent Computer Aided Design (The multi-source analogy generation model in is a quantifiable model, which simulates the process of creative thinking to a certain extent. First, four common parallel MRI image reconstruction algorithms SENSE, SMASH, GRAPPA and PILS are deeply studied in this paper, and the impact of different reconstruction algorithms and different acceleration factor combinations on the quality of reconstructed images is analyzed. The experimental results show that: neural network recognition through feature level fusion The ability of benign and malignant prostate tumors is improved by at least 10%. This feature level fusion strategy is effective and improves the irrelevance between features to a certain extent.

Keywords: Functional MRI; Intelligent CAD; Creative Thinking; Art Design.
DOI: https://doi.org/10.14733/cadaps.2023.S8.180-190

1 INTRODUCTION

Since the 1970s, the research on the brain and its operating mechanism has entered a new era. Many disciplines from different fields such as cognitive psychology, neuropsychology, biology, information science, linguistics, pedagogy and philosophy cross each other, forming a new interdisciplinary research discipline-Brain and Cognitive Neuroscience [1]. To meet the needs of fast imaging, the performance of gradient field has been greatly enhanced, but at the same time, new problems have arisen, and the cost of gradient hardware system is getting higher and higher [2]. In addition, too high gradient field switching rate will cause neuromuscular electromagnetic stimulation. The improvement of imaging speed, which depends on the performance of gradient field, has reached the limit. Clinically, more effective methods are expected to improve the imaging speed. At present, functional MRI (fMRI) of the brain has become the main means to

study the advanced functions of the brain, which promotes people to know the brain more completely, so as to better protect the brain, explore more brain mechanisms and fully develop our brain [3].

All these methods need to calculate the spatial sensitivity of each coil, so as to eliminate the influence of K space under-sampling on image reconstruction. The coil sensitivity can be calculated by obtaining the low-resolution K-space data of each coil and body coil through reference scanning, or by additional scanning K-space lines during calibration. Additional scanning time is added for reference scanning, which is easy to cause motion artifacts and difficult to obtain ideal array coil sensitivity [4]. Creative thinking is a kind of dynamic activity. In the process of creation, it has a clear purpose and direction. When designing, we should give full play to creativity and give it new vitality by basing on the existing wisdom and experience. And make the designer's thinking and ability continue to play. Innovative thinking is based on China's continuous discovery of problems and new deficiencies. We should give full play to our subjective initiative to find new footholds, establish new connections and explore ways to solve problems [5].

In order to solve the above problems, this paper proposes a Neural Network (NN) based on principal component analysis (PCA) for MRI prostate tumor CAD model. By extracting six kinds of features of MRI prostate tumor ROI, 102-dimensional feature vectors are obtained, and on this basis, feature level fusion is carried out to improve the accuracy of prostate tumor CAD diagnosis. The neural network is used to verify the model. The experimental results show that this method is effective, reduces the correlation between features to some extent, and has positive significance for the CAD of MRI prostate tumors. Its innovation lies in:

In the experiment of creative thinking in art design, due to the limitations of experimental conditions, it is not convenient to conduct creative activities when collecting brain images. Therefore, the current solution is to let the subjects imagine how to create during the scanning process. After the scanning, let the subjects recall the creation results and draw or write them. It enables the subjects to create in the scanning process, and designs a face design system based on intelligent computer aided design, so that creative thinking can be quantitatively analyzed.

2 RELATED WORK

Sauli et al. [6] proposed the method of combining TRIZ with CAD design analysis. The modeling is helpful to solve the key problems. In CATIA software, the CAD model of mobile satellite platform shear lift is designed, and ABAQUS is used for analysis to analyze the structure and find out the design problems, and then TRIZ innovation tool is used for optimization. Wendrich [7] introduced the early research and test bed of artificial intelligence technology, which combines creative artificial intelligence (CAI) with hybrid design tools (HDT), environment (HDTE) Make use of rich materials to carry out art education for engineering students at any time. Image processing mainly refers to the process of re-creation such as inputting the externally collected images into the computer for modification. It was difficult to do this in the past. As one of the most successful multimedia tools in the digital media and creative industry, the computer-aided drawing system helps users to convert the input real photos into picturesque images. Xie et al. [8] proposed a stroke-based web collaborative learning and rendering (WebSBLR) system. Unlike the existing methods that mainly focus on art filters, we focus on the stroke rendering engine of client browsers using WebGL and HTML5. The experiment shows that our method is effective for multi-screen painting simulation based on network. It can successfully learn the artist's style and render pictures with consistent and smooth strokes. Yang and Ren [9] helps designers quickly learn design ideas and process image data through this image processing, so as to improve the effect of art design. For example, designers can directly import the image into the computer by scanning or directly copying the data, and then directly process the image. Through Photoshop software, you can directly cut, copy and adjust the picture, or directly convert it into a hand-drawn picture, so as to realize the secondary creation of the image. Image processing mainly refers to the process of re-creation such as inputting the externally collected images into the computer for modification.

Zhao et al. [10] directly adjusts the picture through software, or directly converts it into hand-drawn drawings, so as to realize the secondary creation of images. This kind of image processing can help designers quickly realize the learning of design ideas and the processing of image data, thus improving the effect of art design.

3 METHODOLOGY

3.1 Overview of Functional MRI Technology and Related Theories

The early brain science research was to study the function and structure of the brain through behavioral analysis, autopsy and other means to try to find the junction of function and structure. With the emergence and development of medical imaging technology, the analysis of brain imaging in vivo under non-invasive conditions has been realized. The application of brain imaging technology has promoted the development of brain science and cognitive neuroscience, enabling people to speculate the mystery of the brain black box from the original imagination to spy on the real-time activities of the brain. When using MRA for diagnosis, it is very important to accurately measure the degree of stenosis of blood vessels for clinical diagnosis. It is generally believed that only when the image resolution is high enough, can the stenosis degree of blood vessels be measured with a small error. For the clinical problem of carotid stenosis, since the diameter of the main carotid artery and the diameter of the middle cerebral artery are usually less than 4-8mm and 4mm, a plane resolution of 0.5mm is required for data acquisition to accurately measure the degree of carotid stenosis, which requires a long acquisition time. The generalized FMRI of magnetic resonance functional imaging mainly includes perfusion-weighted imaging, diffusion-weighted imaging and diffusion tensor imaging, magnetic resonance spectroscopy, and blood oxygen level-dependent imaging. In recent years, FMBI-BOLD method has become the most commonly used method, because it is a non-invasive, non-radioactive, high spatial resolution, high temporal resolution, and can accurately locate the functional areas of the brain. It is widely used in cognitive neurological and psychological research such as localization of the functional cortex of the brain, as well as clinical applications such as neurosurgery and neurology.

With this feature, under the guidance of relevant medical knowledge and radiologists, Hu moment invariant features, Tamura texture features, GLCM texture features and frequency domain features of MRI prostate ROI are extracted. As shown in Figure 1.

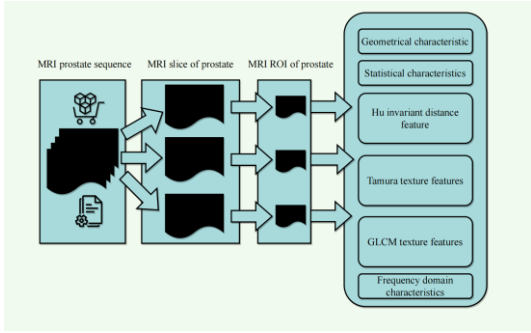

Figure 1: MRI prostate tumor ROI feature extraction process.

The so-called functional MRI technology is based on the paramagnetic sensitivity effect of deoxyhemoglobin. It uses deoxyhemoglobin as a natural contrast agent to achieve complete non-invasive, and the data acquisition process is simple to operate, and can image the whole brain, so it has significant advantages in imaging. In general, communities are also called groups, clusters,

modules, and so on. In social networks, communities may represent groups composed of people with the same topic of interest or background. On the Internet, communities may represent loops and other functional groups in websites and web pages composed of relevant forums.

3.2 Parallel MRI Image Reconstruction Method

In order to improve the imaging speed, parallel MRI adopts multi-element coil array and under-samples K space. At this time, the data of each coil is directly Fourier transformed to obtain a partial FOV image with overlapping of each coil. To obtain a full FOV image without overlapping, a special reconstruction algorithm is needed for image reconstruction. Collect all K-space data for reconstruction, thus obtaining a complete image. When multi-coil parallel imaging technology is adopted, each phased array coil receives signals from the same part of the imaging object at the same time, and respectively obtains K-space data in under-sampling mode. Because each phased array coil has distinct spatial sensitivity information, the images formed by it have different brightness differences at the same position, which also brings additional spatial position information of the imaging object. Using the spatial sensitivity information of each coil and the data collected by each coil, a complete image can be reconstructed. The sparse transform commonly used in compression is wavelet transform, finite difference transform, etc. These image transform methods are often designed according to the experience of digital image processing and image compression.

The thinnest expression of the image is often in different transform domains, so when MRI scans different patients and different parts, it is difficult to apply the preset sparse transform to all situations. Compared with the number of image blocks, the number of features in the dictionary is small, and each image block can use limited features for linear combination. This process can not only extract common features completely based on the image itself, but also combine the existing sparse transformation, or build a dictionary according to the self-similarity of different sequences of MRI images. There are two kinds of methods to obtain non overlapping images. One is based on the reconstruction of K-space domain. The original K-space data collected by each coil is directly combined to obtain full K-space data, and then Fourier transform is performed to obtain full FOV non overlapping images, such as SMASH and GRAPPA. The other is based on image domain reconstruction. Overlapping images obtained from each coil Fourier transform are expanded and combined to obtain full FOV non overlapping images, such as SENSE and PILS. The two kinds of reconstruction algorithms can be expressed in a unified mathematical framework. As shown in Figure 2.

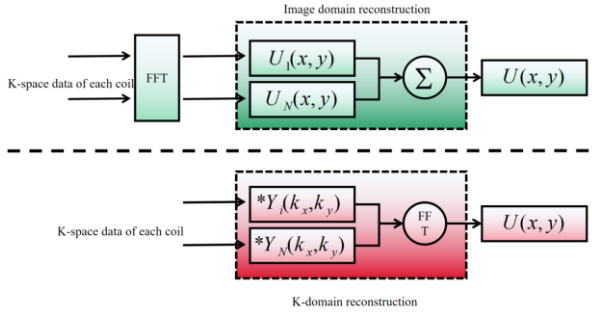

Figure 2: Schematic diagram of parallel MRI image reconstruction.

GRAPPA reconstruction is a more general image reconstruction method based on K-space domain. It is developed on the basis of VD-AUTO-SMASH reconstruction method. Although the two methods have the same way of collecting K-space data, their ways of reconstructing K-space missing data

rows are quite different. GRAPPA no longer fits the data of each array coil to the combined signal, but to the ACS line of a single coil, thus obtaining a series of linear weights to reconstruct the missing K-space data line of each array coil, namely:

$$S^{ACS}{}_i(k_x+m\Delta k_x,k_y)=\sum_{i=1}^{N_c} n^{(m)}{}_i I_i(k_x,k_y) \tag{1}$$

$$I_i(k_x+m\Delta k_x,k_y)=\sum_{i=1}^{N_c} n^{(m)}{}_i I_i(k_x,k_y) \tag{2}$$

In practical applications, camera models are nonlinear models, because the lens is distorted, resulting in errors between the geometric relationship of imaging and the description of the linear model in the actual imaging process. Especially for wide-angle lens, the image at the edge has great distortion. These distortions mainly come from radial distortion and tangential distortion, of which radial distortion is the main source. The error caused by uneven lens and uneven thickness is as follows:

$$\hat{x}=x+x[k_1(x^2+y^2)+k_2(x^2+y^2)^2+k_3(x^2+y^2)^3] \tag{3}$$

Among them, m is the number of pixels overlapping to (x,y), $m=0,1,...,R-1$, and the maximum overlapping number of pixels is R, which is the scanning acceleration factor in the phase coding direction. No more than the number of coils N_c, Fov_x is the overlapping image field of vision in the phase coding direction, and $\eta_i(x+mFov_x,y)$ is the pixel noise at $(x+mFov_x,y)$.

Before using various parallel MRI image reconstruction algorithms to reconstruct images, the sensitivity of each coil must be estimated in advance. After the spatial distribution of the sensitivity of each coil is known, the corresponding weight is given to the contribution of different coils in subsequent image reconstruction, and finally a complete image is reconstructed.

In addition, the mean square sum of the low resolution full FOV image obtained by the array coil itself can also be used as the reference image. This method does not require a separate body coil reference scan, and the calculation is simple. At this time, the calculation formula of coil sensitivity is:

$$\hat{S}_{i\_coil}(x,y)=\frac{I_{i\_coil}(x,y)}{\sqrt{\sum_{i=1}^{N_c}[I_{i\_coil}(x,y)]^2}} \tag{4}$$

$$\theta=\sqrt{2\ln(N)}\cdot\sigma \tag{5}$$

Where n represents the total number of pixels in the image, and σ is the noise standard deviation. For the estimation of signal noise variance, Donoho proposed robust median estimation:

$$\hat{\sigma}=\frac{median(|x_i|)}{0.6255}, x_i\in HH_1 \tag{6}$$

In the actual calibration process, appropriately increase the number of images collected and the angle difference each time is relatively large, which can improve the accuracy. In theory, the more the number of images is, the better. However, too much will increase the amount of calculation and reduce the efficiency of the system. Therefore, to balance the accuracy and system efficiency, we collected images from different angles for calibration. The re projection method is used to check the accuracy of calibration: according to the internal and external parameters obtained from

calibration, the image coordinates of all corners are calculated and compared with the actual corresponding corners. As shown in Table 1.

No.	*Left camera*	*Right camera*
1	0.3655	0.2985
2	0.2658	0.1566
3	0.2658	0.2854
4	0.2954	0.2877
5	0.3025	0.2963
Overall error	0.2515	0.2899

Table 1: Calibration reprojection average error.

The reasons for the analysis error are as follows: (1) The light in the magnet room is not good enough; (2) Interference of magnetic field to camera; (3) The camera is too far from the calibration board. (4) The calibration board is A4 printed chessboard, which is poorly made. But overall, the error is within 1 pixel, which has high accuracy.

3.3 Research on Creative Thinking Based on Intelligent System

According to the multi-source analogy generation model, we hope to develop a face generation system, which takes three face images as analogy sources and generates a new face image by adjusting and combining the parameters of facial features and other attributes, but it can't meet the programming requirements of the experiment. We select some key feature points to present a two-dimensional face, mainly selecting facial features such as face, hair, eyebrows and eyes as the attributes of the analogy source face. The selected feature points will be presented in real time on the right picture. During presentation, the feature points will be fitted with a third-order Bezier curve, and these individual points will be connected to form a continuous curve, so that the image is as realistic as possible. In the research on the brain mechanism of creative thinking, more research is focused on divergent thinking, epiphany and other thinking components, while the research on artistic design creation is relatively less. This is mainly because the task of artistic design is more complicated and limited by experimental conditions, so it is impossible to collect brain images while artistic creation. Our face generation program and the program to ensure the synchronization of psychological experiment tasks and scanning are all on a notebook outside the magnet room. The information was transmitted to this notebook, and the synchronization program captured this signal and immediately triggered the face generation program. The experimental stimulus was synchronously displayed on the display of the magnet room through video transmission. The display still borrowed here, because the IFIS keyboard must use the IFIS system to receive the key signal, we modified the joystick and made a small keyboard. As shown in Figure 3.

In each subject, Pearson correlation coefficient between all voxels is calculated by formula, and a symmetric correlation coefficient matrix A is obtained. Then, we use the statistical test method of single sample test to determine the functional connectivity between pixels in the resting state and then determine the connection edge between nodes in the network. The method is described as follows.

Assuming that the population X obeys $X_1, X_2, \cdots, X_n$ is a sample from X. Their sample average is

$$\overline{X}=\frac{1}{n}\sum_{i=1}^{n}X_i \tag{7}$$

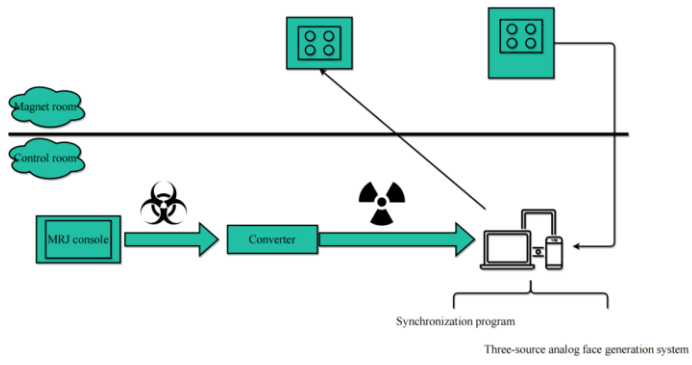

Figure 3: Experimental stimulation platform independent of IFIS.

And the sample variance is

$$S^2=\frac{1}{n-1}\sum_{i=1}^{n}(X_i-\overline{X})^2 \tag{8}$$

When the variance of population X is unknown σ^2, test

$$H_0:\mu=\mu_0,\qquad H_1:\mu\neq\mu_0 \tag{9}$$

Deny domain of. S^2 is an unbiased estimate of σ^2, using

$$t=\frac{\overline{X}-\mu_0}{S/\sqrt{n}} \tag{10}$$

As a test statistic, the rejection field of H_0 is

$$|t|=\left|\frac{\overline{x}-\mu_0}{s/\sqrt{n}}\right|\geq k \tag{11}$$

When H_0 is true,

$$\frac{\overline{X}-\mu_0}{S/\sqrt{n}}\sim t(n-1) \tag{12}$$

In matrix A, a_{ij} represents the correlation coefficient between voxel i and voxel j, and there are 26 samples in a_{ij} among the 26 correlation coefficient matrices, that is, $(a_{ij},1,a_{ij},2,\ldots,a_{ij},26)$. Here, we only consider the positive correlation of the connection, and carry out the right-hand test on the sample. Under the significance level of a, let

$$H_0:\mu\leq T,H_1:\mu>T \tag{13}$$

μ is the sample mean, and T is the closed value of the specified correlation coefficient. Use $t = \frac{\overline{X} - T}{S / \sqrt{n}}$ as the test statistic, and the rejection field of H_0 is

$$t = \frac{\bar{x} - T}{s / \sqrt{n}} \geq t_a(n-1) \tag{14}$$

$$Loss = 1 - (0.5 \times \frac{P \bigcap L}{P \bigcup L} + 0.5 \times \frac{P \bigcap L}{L}) \tag{15}$$

4 RESULT ANALYSIS AND DISCUSSION

In this chapter, the effects of different reconstruction algorithms and different combinations of acceleration factors on the reconstruction results are analyzed when the original MRI data are reconstructed in parallel, and the reconstruction speeds of different algorithms are compared under the condition of fixed acceleration factors. The improved sensitivity calculation method is introduced into automatic calibration SENSE reconstruction, and the influence of different ACS lines and smoothing methods on reconstruction results is analyzed. The quality of reconstructed images before and after sensitivity improvement is analyzed and compared. GRAPPA and SENSE have the best reconstruction effect, SMASH has the second reconstruction effect, and PILS has the worst reconstruction effect. When the acceleration factor becomes larger, the reconstruction effect of all algorithms becomes worse, but at the same time, we can also notice that GRAPPA and SENSE have little change and good stability. As shown in Table 2.

Image algorithm	*reconstruction*	*SENSE*	*SMASH*	*GRAPPA*	*PLLS*
R=2	Noise power	0.002	0.0255	0.0103	0.026
	Reconstruction time	18.25	7.7225	165.255	37.942
R=4	Noise power	0.26164	0.0091	0.05112	0.2612
	Reconstruction time	12.3265	6.2634	130.625	34.102

Table 2: Comparison of reconstruction performance of different algorithms.

From Table 2, we can see that when the acceleration factor is the same, the noise power of GRAPPA and SENSE is the smallest, the noise power of SMASH is the second, and the noise power of PILS is the largest. When the acceleration factor increases, the noise power of all algorithms increases, which is consistent with the results of reconstructed image analysis. In terms of reconstruction speed, when the acceleration factor is the same, SMASH has the fastest reconstruction speed, followed by SENSE and PILS, and GRAPPA has the slowest reconstruction speed. There is a compromise between image reconstruction quality and speed, and SENSE has the best performance.

The experiment shows that, except for T2 weighted images and ADC, when the sequence contains a high b-value DWI, AUC can reach the highest of 0.944, and the 95% confidence interval is 0.876-0.994; But when the sequence does not contain DWI sequence, AUC is only 0.853, and

95% confidence interval is 0.750-0.943; If the sequence contains multiple DWI sequences, the AUC has 0.905, and the 95% confidence interval is 0.816-0.971. These results were statistically compared. It was found that T2-ADC-DWI (b=800s/mm2) had the highest AUC, with a p value less than 0.001. As shown in Table 3.

	Traditional prediction		*Enhanced prediction*	
	PCa	NC	PCa	NC
PCa	22	3	17	2
NC	6	27	5	26

Table 3: Confusion matrix of the same data in the same model using traditional prediction method and enhanced prediction method.

This experiment uses decision analysis curve to compare the results of traditional PI-RADS, deep learning model and their linear combination. The results are shown in Figure 4, Figure 5, Figure 6 and Figure 7. The decision benefit performance of the deep learning model is similar to that of the traditional PI-RADS, but when the two results are combined, the decision curve is shown in the range of risk threshold probability from 5% to 80%, and the combined decision benefit is significantly higher than the two.

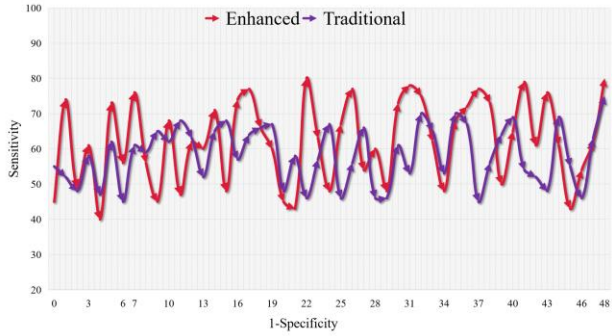

Figure 4: ROC curve comparison between traditional forecasting method and enhanced forecasting method.

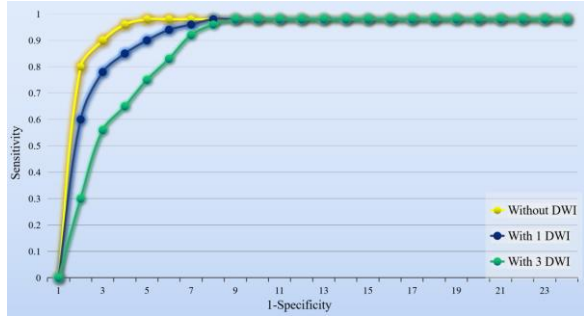

Figure 5: Comparison of ROC curves of different sequence combinations for deep learning model prediction.

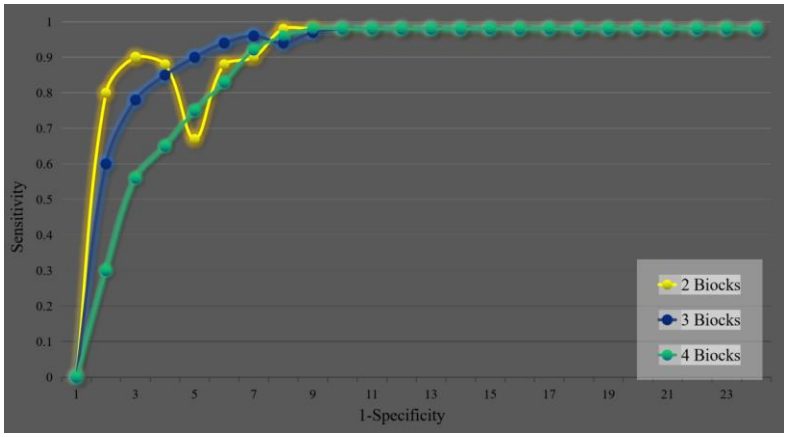

Figure 6: Comparison of ROC curves of different network structures for deep learning model prediction.

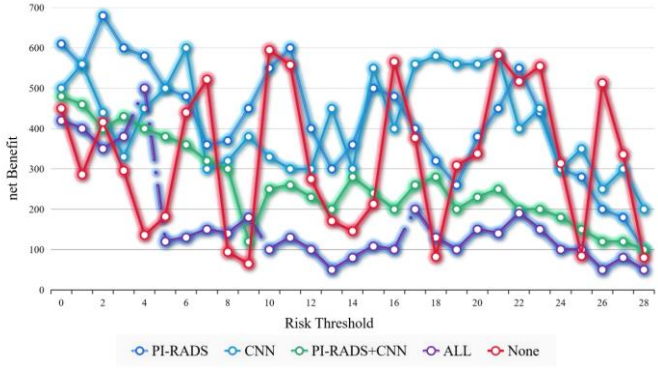

Figure 7: Analysis of Decision Curve of Traditional PI-RADS System and Deep Learning Model.

5 CONCLUSIONS

Magnetic resonance imaging, as a non-invasive image detection technology, has attracted wide attention in medical diagnosis and basic research. However, the imaging speed limits its application in many clinical situations, such as real-time imaging of cardiovascular system and brain function imaging. Common post-processing methods can remove some slight motion artifacts, but it is still difficult to remove large motion artifacts and image processing at scanning level. Magnetic resonance imaging is a commonly used medical image examination method. Its long scanning time and complex reconstruction algorithm provide space for the exertion of artificial intelligence, and its rich contrast information makes it possible for computer-aided diagnosis based on artificial intelligence. With the continuous improvement of image quantity and quality in the era of big data, artificial intelligence technology has broad application prospects in the field of MRI. In this paper, an intelligent analogical generation model is used to write a human face generation software, and an experimental task platform is developed to enable subjects to create faces in the process of collecting brain images. Compared with PI-RADS system, our model can obtain similar performance, and the combination of the two can further improve the diagnostic accuracy.

Yunxia Qu, https://orcid.org/0000-0002-8645-9124
Nan Zhao, https://orcid.org/0000-0002-8645-9124

REFERENCES

[1] Camburn, B.; Arlitt, R.; Anderson, D.; Sanaei, R.; Raviselam, S.; Jensen, D.; Wood, K.-L.: Computer-aided mind map generation via crowdsourcing and machine learning, Research in Engineering Design, 31(4), 2020, 383-409. https://doi.org/10.1007/s00163-020-00341-w
[2] Ekströmer, P.; Wever, R.: "Ah, I see what you didn't mean" exploring Computer Aided Design tools for design ideation, The Design Journal, 22(sup1), 2019, 1883-1897. https://doi.org/10.1080/14606925.2019.1595031
[3] Haghighat, H.; Mirzarezaee, M.; Araabi, B.-N.; Khadem, A.: A sex-dependent computer-aided diagnosis system for autism spectrum disorder using connectivity of resting-state fMRI, Journal of Neural Engineering, 19(5), 2022, 056034. https://doi.org/10.1016/j.bspc.2021.103108
[4] Jeong, A.-C.: Developing computer-aided diagramming tools to mine, model and support students' reasoning processes, Educational Technology Research and Development, 68(6), 2020, 3353-3369. https://doi.org/10.1007/s11423-020-09826-w
[5] Ninga, Z.: Research on the application of computer aided Design in clothing Design teaching in higher vocational colleges, Turkish Journal of Computer and Mathematics Education (TURCOMAT), 12(3), 2021, 4817-4821. https://doi.org/10.17762/TURCOMAT.V12I3.1985
[6] Sauli, S.-A.; Ishak, M.-R.; Mustapha, F.; Yidris, N.; Hamat, S.: Hybridization of TRIZ and CAD-analysis at the conceptual design stage, International Journal of Computer Integrated Manufacturing, 32(9), 2019, 890-899. https://doi.org/10.1080/0951192X.2019.1644536
[7] Wendrich, R.-E.: Computer aided creative thinking machines (Caxtus), Computer-aided design and applications, 18(6), 2021, 1390-1409. https://doi.org/10.14733/cadconfP.2020.81-85
[8] Xie, N.; Zhao, T.; Yang, Y.; Shen, H.-T.: Web-based SBLR method of multimedia tools for computer-aided drawing. Multimedia Tools and Applications, 78(1), 2019, 799-816. https://doi.org/10.1007/s11042-018-5949-x
[9] Yang, Y.; Ren, H.: The Teaching Method Combining Art Design and CAD Design, Computer-Aided Design and Applications, 19(S8), 2022, 157-167. https://doi.org/10.14733/cadaps.2022.s8.157-167
[10] Zhao, Y.; Samuel, R.-D.-J.; Manickam, A.: Research on the application of computer image processing technology in painting creation, Journal of Interconnection Networks, 22(Supp05), 2022, 2147020. https://doi.org/10.1088/1742-6596/1915/3/032050